INTERNATIONAL SOCIETY FOR
SOIL MECHANICS AND
GEOTECHNICAL ENGINEERING

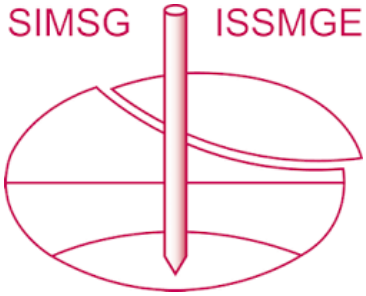

This paper was downloaded from the Online Library of the International Society for Soil Mechanics and Geotechnical Engineering (ISSMGE). The library is available here:

https://www.issmge.org/publications/online-library

This is an open-access database that archives thousands of papers published under the Auspices of the ISSMGE and maintained by the Innovation and Development Committee of ISSMGE.

The paper was published in the proceedings of the 10th International Conference on Scour and Erosion and was edited by John Rice, Xiaofeng Liu, Inthuorn Sasanakul, Martin McIlroy and Ming Xiao. The conference was originally scheduled to be held in Arlington, Virginia, USA, in November 2020, but due to the COVID-19 pandemic, it was held online from October 18th to October 21st 2021.

On the Mechanics of Internal Erosion in Cohesionless Soil

Maoxin Li[1], Ph.D., P.Eng. and Jonathan Fannin[2], Ph.D., P.Eng.

[1]British Columbia Hydro and Power Authority, Senior Geotechnical Engineer, Burnaby, BC, Canada; e-mail: maoxin.li@bchydro.com
[2]University of British Columbia, Professor of Civil Engineering, Vancouver, BC, Canada; e-mail: jonathan.fannin@ubc.ca

ABSTRACT

Erosion by internal instability refers to seepage flow moving finer particles through the primary pore network of the soil. Empirical methods are available to screen for gradation susceptibility, however there is need to develop a mechanics-based understanding of the phenomenon. The onset of instability in sand and gravel specimens was examined using two rigid-wall permeameters, of different size, in testing at different vertical effective stress and hydraulic gradient. The onset of internal instability in a soil is found to be governed by a hydromechanical envelope, defined as a linear relation between the normalized vertical effective stress and critical hydraulic gradient. The slope of the envelope is associated with the Skempton-Brogan stress reduction factor, α. The influence of scale effect is examined in the test results. In tests with upward flow, a distinction is made between internal instability and heave failure. The combined influence of seepage direction, hydraulic gradient, and effective stress, is unified within the context of a mechanics-based understanding of erosion by internal instability.

INTRODUCTION

Risk management in dam engineering must consider the consequences of failure, and the uncertainty associated with each failure mode. Embankment dam failures are generally attributed to (i) erosion by overtopping, (ii) slope instability, and (iii) internal erosion. Seepage-induced internal erosion has recently been categorized with reference to several distinct mechanisms (ICLOD, 2017, USBR/USACE, 2018). Internal instability refers to the erosion of finer particles from the soil gradation through its primary pore network, under the influence of seepage flow. It occurs in broadly-graded or gap-graded soils that exist in natural deposits, and also in engineered-fill structures such as embankment dams and levees. Erosion of fine particles could reduce the soil permeability due to clogging, increased pore water pressures, and a deterioration of the filter and drainage system (Sterpi, 2003). It could also yield changes in gradation that affect the load-deformation properties of a soil and result in potential for volumetric collapse of the soil. Erosion by internal instability is one of main reasons for dam incidents/failures involved widely graded glacial soils (Sherard, 1979, Foster et al., 2000, USBR/USACE, 2018). It serves to emphasize the importance of seepage analysis, and the need for rational design methods, in dam engineering.

There are several empirical methods to evaluate the material susceptibility to internal instability (Kezdi, 1979, De Mello 1975, Sherard, 1979, Kenney and Lau, 1985, 1986, Burenkova, 1993, Wan and Fell, 2008, Li and Fannin, 2008, Indraratna et al. 2011, Li and

Fannin 2013). Empirical methods provide a screening-tool to evaluate the potential susceptibility of a soil gradation, however they are not a substitute for rational design methods. Accordingly, there is need to develop a mechanics-based understanding of the internal instability phenomena. A greater understanding of the instability mechanics will address two questions for potentially unstable soils: (1) what conditions trigger the internal instability, i.e., where is the susceptibility to onset of internal instability; (2) what is the effect of internal erosion on the soil properties, i.e., over what period time might that susceptibility manifest itself.

In a susceptible material, the onset of instability is governed by factors including effective stress and hydraulic gradient (Moffat and Fannin, 2011). Yet these influences are not well understood. Skempton and Brogan (1994) examined the response of four sandy gravels to upward flow. They found internally unstable sandy gravels failed at a roughly 1/3 to 1/5 of the theoretical vertical gradient of approximately 1.0. Similar experimental tests were reported by Wan and Fell (2004), Liu (2005) and Mao (2005). Skempton and Brogan postulated that the distribution of effective stress in a specimen may influence potential of internal instability. Moffat and Fannin (2006, 2011) first studies the effect of vertical effective stress on the onset of internal stability of four cohesionless materials. They found that the critical gradient proportionally increases with the increasing of the vertical effective stress. In this paper, the onset of instability in sand and gravel specimens is examined using two rigid-wall permeameter, of different size, in testing across a range of vertical effective stress and hydraulic conditions. The findings serve to advance a mechanics-based understanding of seepage-induced internal erosion, and in support of more rational design methods to complement empirical screening tools.

EXPERIMENTS

Five different materials were tested: one was internally stable and four were potentially unstable. The test gradations are shown in Figure 1, and characteristics of the gradation size distribution are reported in Table 1. The geometric index $(D'_{15}/d'_{85})_{max}$ from the split method (Kezdi, 1979) and $(H/F)_{min}$ from Kenney and Lau (1985, 1986) are also shown in Table 1.

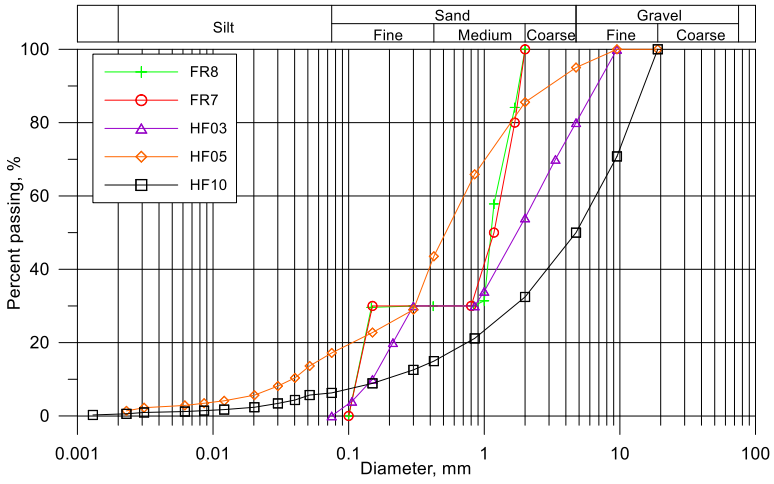

Figure 1 Grain size distribution curves of the test specimens

Two permeameters were used in the experiments. The relatively small permeameter was originally designed for assessment of soil-geotextile filtration compatibility at UBC (Fannin et al., 1996). The permeameter cell assembly is submerged in an outlet tank made of Plexiglas. A photograph of the entire cell assembly is shown as Figure 2, together with a schematic drawing of the assembly. The permeameter cell is made of anodized aluminum, with an inner diameter of 102 mm.

Table 1 Characteristics of the test gradations

Gradation	D_{10} (mm)	D_{30} (mm)	D_{50} (mm)	D_{60} (mm)	C_u	C_c	$(D'_{15}/d'_{85})_{max}$	$(H/F)_{min}$	Wire mesh (mm)	Lab. results
FR8	0.119	0.150	1.219	1.346	11.3	0.1	7.9	0	0.6	U
FR7	0.119	0.150	1.118	1.327	11.2	0.1	7.1	0	0.6	U
HF03	0.150	0.300	1.741	2.427	16.2	0.2	4.9	0.3	1.14	U
HF05	0.027	0.238	0.425	0.601	22.2	3.5	5.5	0.5	1.14	U
HF10	0.185	1.662	4.750	6.637	35.9	2.2	-	0.98	1.14	S

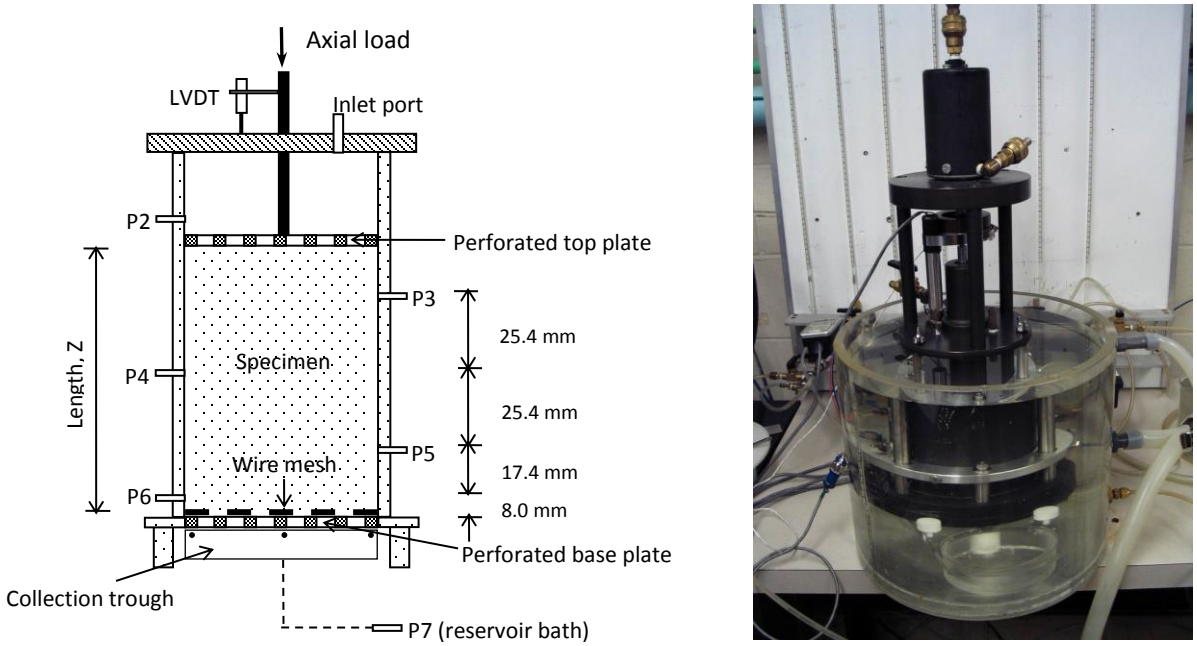

(a) (b)

Figure 2 The small permeameter: (a) schematic drawing; (b) test device

The large permeameter was specifically designed at UBC for the assessment of internal stability in soils of the core and transition materials of the WAC Bennett dam (Moffat and Fannin, 2006). A photograph of the permeameter cell assembly is shown in Figure 3, together with a schematic drawing of it. The permeameter cell is made of acrylic, with an inner diameter of 279 mm. The maximum grain size of test specimens in the small and larger permeameters was

restricted to 8 and 23 mm, respectively, giving a ratio of cell diameter to largest particle size greater than 10 (Kenney et al, 1985, ASTM D5101, 1996).

The specimen was prepared using the modified slurry deposition method (Kuerbis and Vaid, 1988; Moffat and Fannin, 2006). The specimen was reconstituted in a series of layers. Each batch of materials was boiled in clean de-aired water and then placed under vacuum to remove any entrained air. The material was deposited under a thin layer of standing water to ensure a saturated specimen and minimize segregation. A vertical load was applied on the top of specimen to consolidate the specimen to the target vertical stress. The hydraulic gradient was increased gradually in multiple stages in order to identify the critical hydraulic gradient at which erosion initiates. Details of the experiments can be found in Li (2008). The reconstitution method is an alternative to that of moist-tamping (or wet compaction), which is commonly used in other studies.

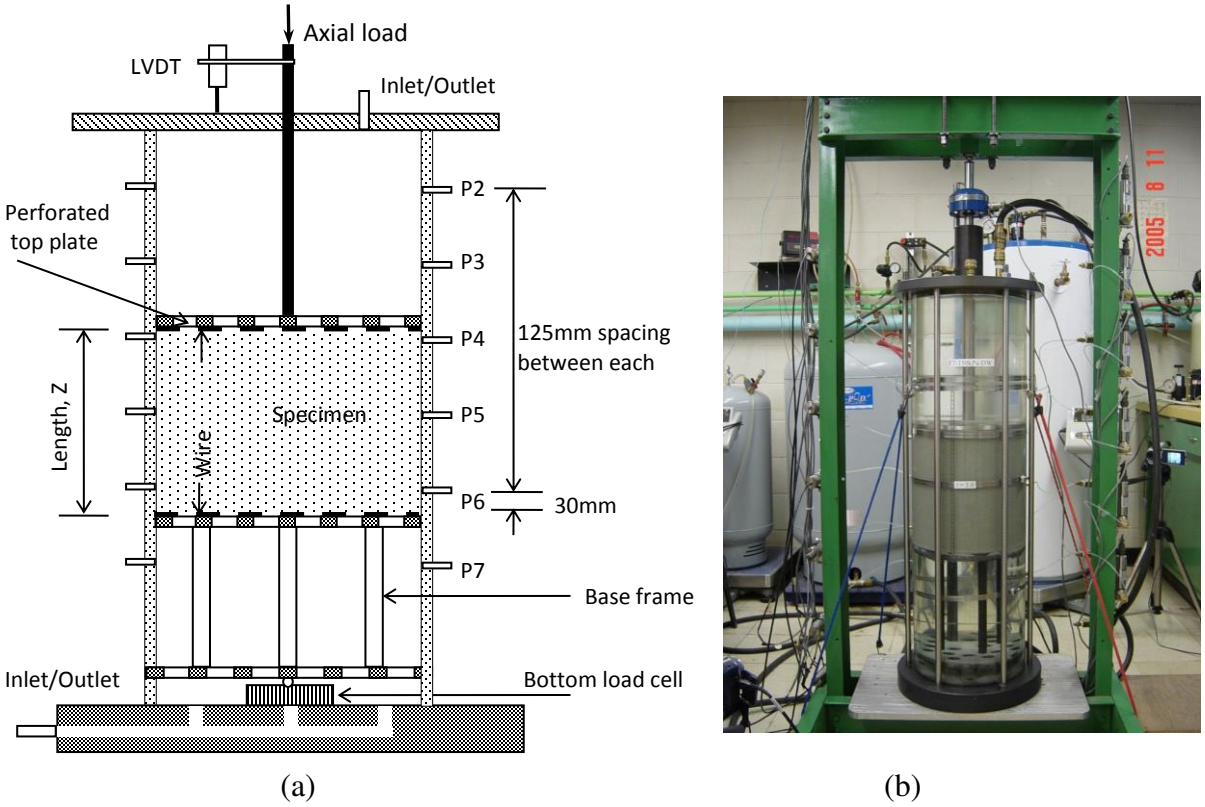

Figure 3 The large permeameter: (a) schematic drawing; (b) test device

RESULTS

Instability Failure and Heave Failure

Internally unstable soils exhibited similar failure behaviors in both upward and downward flow tests, which generally involved the following phenomena: (1) an increase of seepage velocity, (2) an increase of mass loss, (3) a sudden change in the local hydraulic gradient (i_{jk}, where j and k refer to port locations on the permeameter) and, in some test gradations, (4)

compressive axial strain of the specimen. Typical failure behaviors of an internally unstable soil are shown on Figure 4. The test code defines the gradation, applied stress and flow direction. For example, FR7-50-D represents a test on gradation FR7 with applied stress of 50 kPa in the downward direction.

Consistent with intuitive expectations, the internally stable soil did not experience any failure in tests with downward flow and exhibited heave failure in the upward flow tests. Attention should be given to distinguish between instability failure and heave failure, in tests with upward flow. Typical heave failure behaviors are shown on Figure 5.

It can be seen, from comparison of Figs. 4 and 5, that heave failure involved an increase of seepage velocity and change in local hydraulic gradient, together with an upward displacement (reported as negative strain). In contrast, a downward displacement (reported as positive strain) was observed in an internal instability failure.

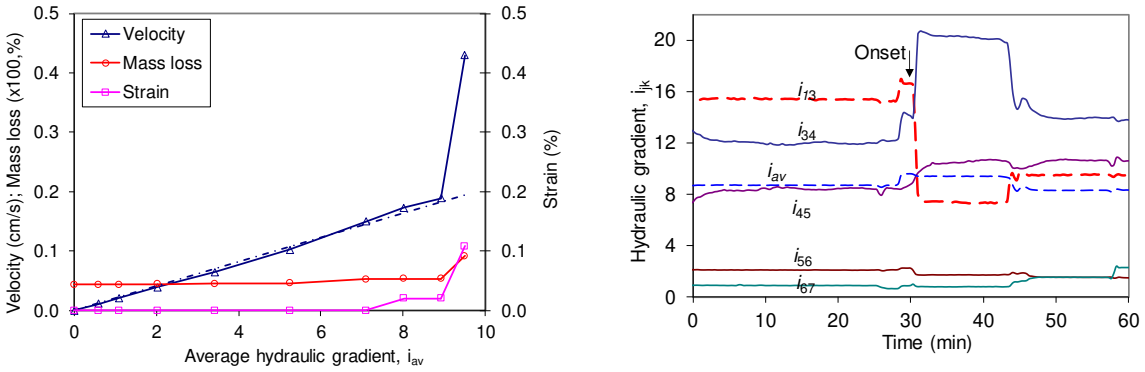

Figure 4 Onset of internal instability failure (FR7-50-D) in small permeameter

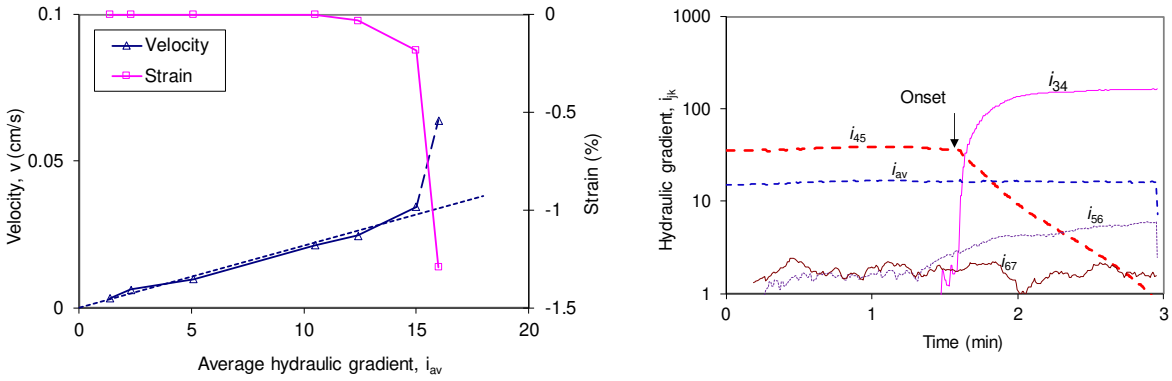

Figure 5 Onset of heave failure (HF10-25-U) in large permeameter

As expected, hydraulic properties of the internally unstable material change because of mass loss. Figure 6 shows the change of permeability after instability failure. It appears the permeability increases with the increase of mass loss and is not dependent on stress levels.

The critical hydraulic gradient is defined herein, and consistent with general usage, as the local hydraulic gradient between two port locations where the onset of any seepage-induced instability failure (in a potentially unstable gradation) or heave failure (in a stable gradation) first occurs. This local layer where the failure first occurs is defined as the “onset layer”. The critical hydraulic gradient can be determined by examining the increase of seepage velocity and/or the

change in local hydraulic gradient as shown on Figures 4 and 5. Variation of effective stress could be deduced using the 1-D piece-wise effective stress model incorporating the measured top and bottom stresses of the tested specimen (Li, 2008).

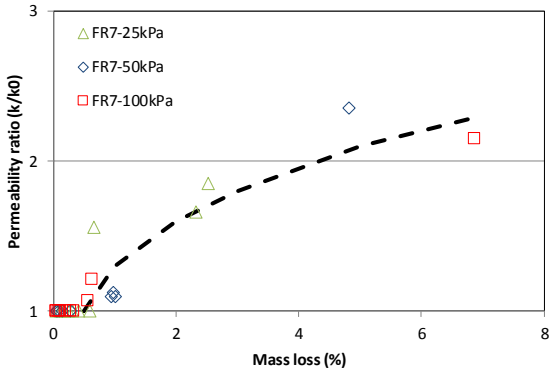

Figure 6 Variation of permeability with mass loss: gradation FR7

Scale effect

Five tests were conducted on the potentially unstable gradation FR7, in both the small and large permeameter. The critical hydraulic gradient in the 'onset layer' (as defined earlier) and mean vertical effective stress in the 'onset' layer, are plotted in Figure 7. A linear relation was observed between critical gradient and mean vertical effective stress in results from the small and large permeameter tests, respectively. Moffat and Fannin (2011) also demonstrated that the critical hydraulic gradient would increase with effective stress based on their observations in the large permeameter tests. However, the relation is not unique: the slope formed in data from the small permeameter tests is much steeper than that from the large permeameter tests. The difference is attributed to scale effects, given the length of the local failure zone between adjacent measurement port locations is about 2.5 cm in the small permeameter and about 12.5 cm in the large permeameter. It indicates that the longer is the specimen, the smaller is the critical hydraulic gradient. This scale effect is believed to associate with the balance of force in a specimen with an overburden. The seepage force in a specimen can be expressed as $i^*r_w^*$volume. For a given hydraulic gradient, the longer specimen, the larger the seepage force in the specimen, therefore a larger applied stress is required to balance the seepage force. For a specimen without an overburden, the scale effect is deemed to be not applicable.

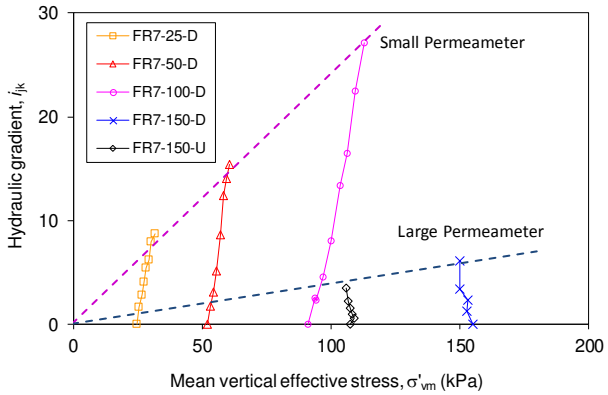

Figure 7 Relation between critical hydraulic gradient and vertical effective stress

To unify the two sets of data, a dimensionless approach was taken to eliminate the scale effect. Li and Fannin (2012) have theoretically demonstrated that the critical hydraulic gradient in the one-dimensional flow case is proportional to the normalized mean vertical effective stress ($\sigma'_{vm}/(\gamma_w \Delta z)$). The data in Figure 7 were re-plotted in Figure 8 using the normalized mean vertical effective stress, together with hydromechanical path, which represents the variation of normalized mean vertical effective stress with local hydraulic gradient (i_{jk}) across the 'onset' layer for each test. They yield a relation between critical gradient and normalized effective stress that appears somewhat unique for the two sets of data.

A scale effect was also observed by Marot et al. (2012) in their experimental study on the suffusion of clayey sand with different sample lengths. They found that the values of the suffusion rate increase linearly depending on the length of the tested sample.

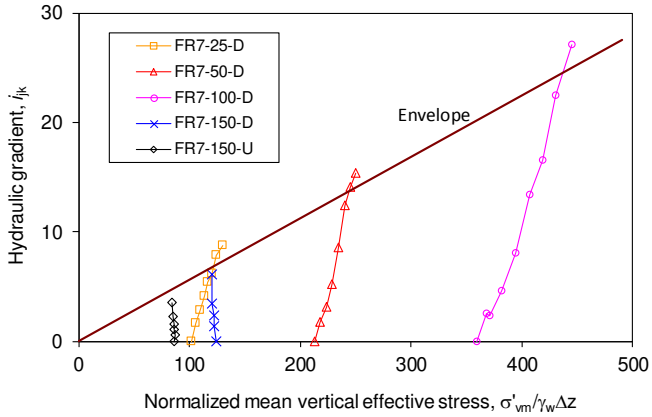

Figure 8 Hydromechanical paths and envelope for gradation FR7

Onset of Internal Stability and Hydromechanical Envelope

As shown on Figure 8, the hydromechanical paths appeared to be bounded by an envelope at which the onset of instability occurs. The envelope is generally defined by a relation between normalized mean vertical effective stress and hydraulic gradient for each gradation (Moffat and Fannin, 2011, Li and Fannin, 2012). The hydromechanical paths for both upward and downward tests on gradation FR7 appear to approach an identical failure envelope, which has significance for a mechanics-based understanding of the erosion mechanism. However, further research needs to shift its investigation to a relation with mean effective stress (by means of flexible-wall permeameter testing, rather than rigid-wall permeameter testing), and to examine the relation between mean effective stress and a critical-state type characterization of strength and deformation (by means of triaxial-permeameter testing). Figure 9a shows the envelope for each of the five tested gradations (see Fig. 1).

The difference in the plotting position of the failure envelope of each gradation is attributed to its susceptibility to erosion (Moffat and Fannin, 2011): the greater the susceptibility to internal instability, the lower the slope of the hydromechanical envelope. Li and Fannin (2012) found that a linear relation between ($\sigma'_{vm}/(\gamma_w \Delta z)$) and i is governed by the stress reduction factor α. The concept of α was first proposed by Skempton and Brogan (1994) and extended by Li and Fannin (2012) in Eq.1:

$$\sigma'_f = \alpha\, \sigma'_{vm} \quad (1)$$

where σ'_f and σ'_{vm} are the effective stresses on finer particles and coarser particles of an internally unstable soil, respectively.

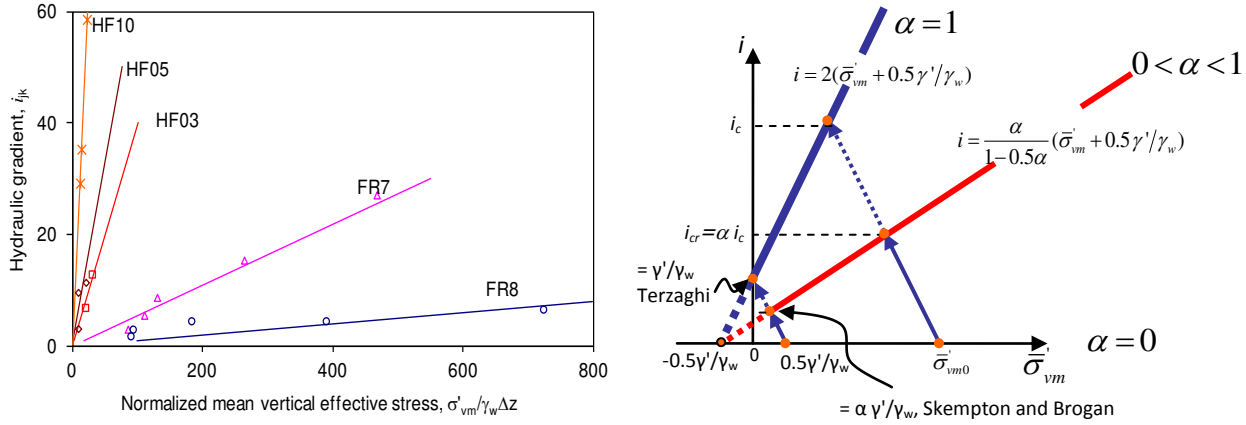

(a) Envelopes for tested specimen (b) Theoretical envelope

Figure 9 Tested and theoretical hydromechanical envelope

The values of α vary from 0 to 1. Skempton and Brogan (1994) postulated the values of α depend on the value of the stability index $(H/F)_{min}$ from Kenney and Lau (1986). Li and Fannin (2016) further investigated the relation between α and geometric indexes, and found a generally good correlation between α and d_0/d'_{85} (coefficient of correlation of 0.74) as shown on Figure 10, and expressed as in Eq.2:

$$\alpha = 3.85/(d_0/d'_{85}) - 0.616 \quad (2)$$

where d_0 is the average pore size of the coarser fraction of a soil proposed by Kovacs (1981).

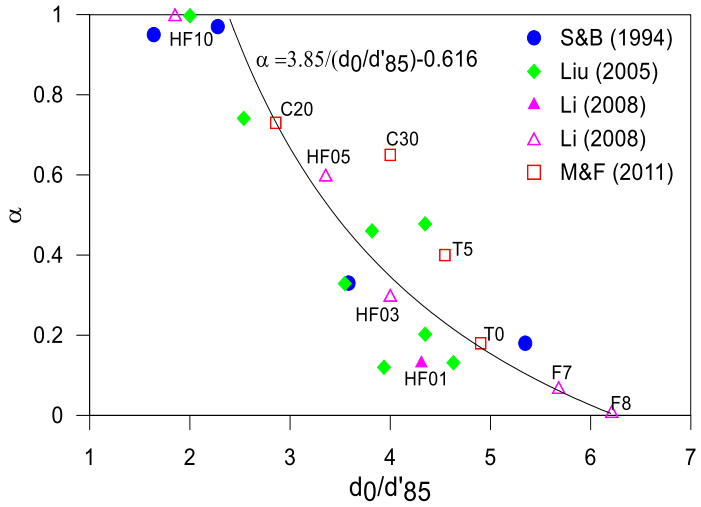

Figure 10 Variations of α with geometrical index (d_0/d'_{85})

Shire et al (2014) have estimated the values of α using the Discrete Element Method (DEM) on gap-graded spheres. They found that soils with a finer fraction of 24% have an α value of about 0.1 and are under-filled, soils with a fines content of 35% or more have an α value of 1.0 and are over-filled. Soils with a finer fraction between 24% and 35% are deemed transitional.

CONCLUSION

Seepage analysis and design of effective measures for its control are essential to risk management in dam engineering. On the matter of failure by internal erosion, there is need to develop rational design methods to complement empirical approaches used in practice. A mechanics-based understanding of the phenomenon serves to inform advances in practice.

The laboratory tests reported herein establish that the onset of internal instability of a soil is governed by a hydromechanical envelope. The envelope is a function of stress reduction factor, α, which is correlated with geometrical indices of the soil gradation. There is a scale effect governing the critical hydraulic gradient associated with onset of instability. For a given loading, the longer is the specimen, the smaller is the critical hydraulic gradient. Internal instability failure of tested specimens associates with an increase of seepage velocity, mass loss and/or volume change. A downward displacement was observed in the instability failure in contrast to an upward displacement in the heave failure. To develop a theoretical model for erosion by internal instability, it is believed crucial to pursue further research on the full erosion process including initiation and post-failure behaviors.

ACKNOWLEGEMENTS

Funding for research on internal stability of soils at the University of British Columbia is provided by NSERC, and the British Columbia Hydroelectric Power Authority.

REFERENCES

ASTM (American Society for Testing and Materials). (1996). *Standard Test Method for Measuring the Soil-Geotextile Clogging Potential by the Gradient Ratio (D5101-96)*. in the Annual Book of ASTM Standards, Vol. 04.09, ASTM Philadelphia, USA.

Burenkova, V. V. (1993). *Assessment of suffusion in noncohesive and graded soils*, in Filters in Geotechnical and Hydraulic Engineering, Eds. Brauns, Heibaum & Schuler, Balkema, 357-360.

De Mello, F.B. (1975). *Some lessons learned from unsuspected, real and fictitious problems in earth dam engineering in Brazil*. 6th Regional Conference for Africa on Soil Mechanics and Foundation Engineering, Durban, S. Africa, 285-304.

Foster, M., Fell, R., and Spannagle, M. (2000). *A method for assessing the relative likelihood of failure of embankment dams by piping*, Can. Geotech. J., 37: 1025-1061.

Indraratna, B., Nguyen, V.T. and Rujikiatkamjorn, C. (2011). *Assessing the potential of internal erosion and suffusion of granular soils*. J. of Geotech. and Geoenv. Engng., 137: 550-554.

Kezdi, A. (1979). *Soil physics – selected topics*. Elsevier Scientific Publishing Company, Amsterdam, 160p.

Kenney, T.C., Chacal R., Chiu, E., Ofeogbu, G.I., Omanga, G.N., and Ume, C.A. (1985), Controlling constriction sizes of granular filters, Can. Geotech. J., 22: 32-43.

Kenney, T.C. and Lau, D. (1985). *Internal stability of granular filters*. Can. Geotech. J., 22: 215-225.

Kenney, T.C. and Lau, D. (1986). *Internal stability of granular filters: Reply.* Can. Geotech. J., 23: 420-423.

Kuerbis, R.H. and Vaid, Y.P. (1988). *Sand Sample Preparation – The Slurry Deposition Method.* Soils and Foundations, 28 (4): 107-118.

Kovacs, G. (1981). *Seepage Hydraulics*. Elsevier Scientific Publishing Company, Amsterdam, 730p.

Li, M. (2008). *Seepage-induced failure of widely-graded cohesionless soils*. Ph.D. thesis, Department of Civil Engineering, The University of British Columbia, Vancouver, B.C.

Li, M. and Fannin, R.J. (2012). *A theoretical envelope for internal instability of cohesionless soil.* Geotechnique 62(1):77-80.

Li, M. and Fannin, R.J. (2013). *A Capillary Tube Model for Internal Stability of Cohesionless Soil*, Journal of Geotech. and Geoenv. Engng, 139: 831-834

Li, M. and Fannin, R.J. (2016). *Critical hydraulic gradients for internally unstable cohesionless soils.* 69th Canadian Geotechnical Conference, GeoVancouver.

Liu, J. (2005). *Seepage control of earth-rock dams theoretical basis, engineering experiences and* lessons (in Chinese). China Waterpower Press, Beijing. 219p.

Mao, C.X. 2005. *Study on piping and filters: Part I of piping (in Chinese).* Rock and Soil Mechanics, 26 (2): 209-215.

Marot, D.,Le, V.D., Garmier, J., Thorel, L., Audrain, P. (2012). *Study of scale effect in an internal erosion mechanism.* European J. of Environmental and Civil Engng., 16(1): 1-19.

Moffat, R. and Fannin, R.J. (2006). *A large permeameter for study of internal stability in cohensionless soils*. ASTM Geotechnical Testing J., 29(4): 1-7.

Moffat, R. and Fannin, R.J. (2011). *A hydromechanical relation governing internal stability of cohensionless soil*. Can. Geotech. J., 48: 413-424

Sherard, J.L. (1979). Sinkholes in dams of coarse, broadly graded soils, in Proc. 13th ICOLD Congress, New Dehli, India. Vol. 2, pp.25-34.

Shire, T.; O'Sullivan, C., Hanley, K. and Fannin, R.J. (2014). *Fabric and effective stress distribution in internally unstable soils*. J. of Geotech. and Geoenv. Engng, 140: 04014072.

Skempton, A.W. and Brogan, J.M. (1994). *Experiments on piping in sandy gravels.* Geotechnique, 44: 449-460.

Sterpi, D. (2003). *Effects of the erosion and transport of fine particles due to seepage flow*, International Journal of Geomechanics, Vol. 3, No. 1, pp.111-122

USBR/USACE (U.S. Bureau of Reclamation/Army Corps of Engineers). (2018). *Best Practices and Risk Methodology – Chapter D-6 Internal Erosion Risks for Embankments and Foundations*.

Wan, C.F. and Fell, R. (2004). *Experimental investigation of internal erosion by the process of suffusion in embankment dams and their foundations*, ANCOLD Bulletin No. 126: 69-78.

Wan, C.F. and Fell, R. (2008). *Assessing the potential of internal stability and suffusion in embankment dams and their foundations*. J. Geotech. & Geoenv. Engng. 134: 401–407.